

# GEOTECHNICAL INVESTIGATION OF A LANDSLIDE INCIDENT IN HULU KELANG, MALAYSIA

\*Jestin Jelani<sup>1</sup>, Muhammad Shafiq Soffian Abdul Rahman<sup>1</sup>, Suriyadi Sojipto<sup>1</sup>, Wan Mohamed Syafuan Wan Mohamed Sabri<sup>1</sup>, Lee Min Lee<sup>2</sup> and Nordila Ahmad<sup>1</sup>

<sup>1</sup>Civil Engineering Department, National Defence University of Malaysia, Malaysia

<sup>2</sup>Civil Engineering Department, University of Nottingham Malaysia, Malaysia

\*Corresponding Author, Received: 10 July 2023, Revised: 02 June 2024, Accepted: 05 June 2024

**ABSTRACT:** Malaysia is located in a tropical region and receives high rainfall intensity, especially during the monsoon season, which is often associated with landslide disasters. This study conducted a geotechnical investigation to examine the causative factors of a landslide incident on 18 September 2021 at Kemensah Heights, Hulu Kelang, Selangor, Malaysia. The landslide was triggered after three days of rainfall and shifted approximately 2536 m<sup>2</sup> of land, affecting three bungalows and 19 double-story houses located at the top and toe of the slope. The investigation used a combination of a Terrestrial Laser Scanner (TLS) Survey, a Public Work Department Probe Test also known as the JKR Probe Test, laboratory testing, and numerical modeling to analyze the landslide. Soil samples were collected to test grain size distribution, Atterberg limits, permeability, soil density, consolidated-undrained (CU) tri-axial strength, and soil density. The residual soils comprised sand (42%), silt (28%), clay (16%), and gravel (14%), classifying it as 'silty sand'. The average permeability is  $5.96 \times 10^{-3}$  mm/s, indicating medium permeability. The slope angle measured using TLS and a geological compass ranged from 30° to 35°. The cohesion and internal friction angle of the soil is 11.3 kPa and 29°, which are less than the slope angle, indicating that the slope is susceptible to landslides. Numerical simulation analysis, using Plaxis 3D and Slope/W, was carried out to determine the factor of safety (FOS). This study concludes that the triggering factors causing the landslide were not only limited to the antecedent rainfall but were also due to excessive imposed load and the characteristics of the residual soil.

*Keywords: Landslide, Plaxis 3D, Rainfall, Hulu Kelang, Slope/W*

## 1. INTRODUCTION

Landslides are naturally occurring geological hazards in many areas of the world and are caused by the movement of rock or soil down a slope as a result of gravity [1]. Landslides seldom occur because of a single factor; instead, they are the result of a combination of several factors, such as intense rainfall [2,3], seismicity [4], changes in water level [5], excessive imposed load [6,7], steep slope profile [8], anthropogenic factors [9,10], etc. These factors increase shear stress within the soil mass, causing it to exceed the shear strength of the soil. The vulnerability of an area to landslides (from a residential and commercial point of view) expands into precarious slope regions to fulfill the demand of population growth and urbanization, thus exacerbating this susceptibility.

In Malaysia, rainfall is the primary factor causing landslides. According to the United States National Aeronautic Space Administration (NASA), Malaysia ranks among the top ten countries that are most susceptible to landslides [11]. The vulnerability is particularly evident during the monsoon season when Malaysia receives frequent and prolonged rainfall. Between 1993 and 2011, 28 significant landslides were recorded, 21 of them being triggered by rainfall. The landslides resulted

in more than 100 casualties and economic losses exceeding US \$1 billion [12].

Hulu Kelang is a mature neighborhood located just 10 km from Kuala Lumpur city center. It is well-known as a landslide-prone area due to its hilly and undulating terrain; it is located close to the foot of the Titiwangsa Mountain Range. Since 1993, the Hulu Kelang area has consistently experienced devastating landslides. Most of the landslides took place in developed hillside regions, primarily because the natural slope was disrupted. High demand for residential housing and commercial buildings has brought challenges for developers, and some of them encroached onto highlands in the hilly areas. The situation is exacerbated because Hulu Kelang receives high annual rainfall, with an average of 2400 mm [13]. The combination of these factors contributes significantly to the occurrence of landslides. Table 1 shows the specific locations of historical rainfall-induced landslides in Hulu Kelang from 1990-2011 [2].

Many studies have been conducted by local researchers to determine the main causes of landslides in the Hulu Kelang area. The study by [14] identified inadequate design of retaining structures and slopes as being the primary cause of landslides in Hulu Kelang. The study by [15] supported these findings; they found that improper

design and construction methods were the primary causes of the landslides, such as inadequate support of lateral loads caused by underground land movement. These poorly designed and constructed slopes failed during or after heavy rainfall events. Another potential contributing factor to the landslides was inadequate maintenance of the internal drainage systems of the slopes and retaining structures. Another study conducted by [16] identified 152 landslide scars on both soil and rock slopes, indicating that these slopes are potential slope failure sites. Furthermore, [17] conducted a detailed investigation into one of the major landslides, the 2008 Bukit Antarabangsa landslide, and concluded that the prolonged rainfall during the monsoon season was one of the primary triggering factors.

This paper investigates a recent landslide incident in September 2021 at Kemensah Heights, an area located in part of Hulu Kelang province. The objective of this investigation is to identify the probable causes initiating landslides and the contributing factors. The investigation used a combination of Terrestrial Laser Scanner (TLS) Surveys, JKR probe tests, laboratory testing, and numerical modeling to analyze the landslide.

Table 1 Locations of the historical rainfall-induced landslides in Hulu Kelang from 1990-2011 [2].

No	Location	Date
1	Highland Tower	December 1993
2	Keramat Permai	3 May 1995
3	Keramat Permai	15 May 1995
4	Ampang Jaya	August 1995
5	Ampang Jaya	June 1996
6	Bukit Antarabangsa	14 May 1999
7	Bukit Antarabangsa	15 May 1999
8	Jalan Bukit Antarabangsa	October 2000
9	Taman Zooview	October 2001
10	Taman Zooview	November 2001
11	Taman Hillview	November 2002
12	Bukit Antarabangsa	2 November 2003
13	Bukit Antarabangsa	7 November 2003
14	Dataran Ukay	February 2005
15	Kg Pasir	May 2006
16	Bukit Antarabangsa	April 2008
17	Bukit Antarabangsa	December 2008
18	Bukit Antarabangsa	September 2009
19	Ukay Club Villa	April 2010
20	Bukit Antarabangsa	August 2010
21	Ukay Perdana	February 2011

## 2. RESEARCH SIGNIFICANCE

It is vital to identify and understand the factors causing landslides, and the interactions between them to develop effective measures to stabilize the slope and minimize the impacts of future occurrences. Regarding the landslide incident at Kemensah Heights, there is no investigation or assessment has been documented in the available literature. Hence, this study aims to explore and

analyze the causative factors of landslides at Kemensah Heights through a geotechnical perspective.

## 3. STUDY AREA

The study area extended from latitude N 3° 12.770753' and longitude E 101° 45.861068', with an average elevation of 60-75 m above sea level (Fig. 1). The landslide translated approximately 2536 m<sup>2</sup> of earth, blocking a river downstream of the slope (Fig. 2). The landslide affected three bungalows and 19 double-story houses at the top and toe of the slope and necessitated the evacuation of 28 families. Fortunately, there were no fatalities. The landslide disaster occurred after three days of rainfall. The average rainfall data at the Bukit Antarabangsa station recorded the antecedent rainfall from 15, 17 and 18 September 2021 as being 24, 18, and 13 mm/hr (and 18 and 6 mm/hr on 19 and 20 September 2021 (Fig. 3)). According to the local experts, the rainfall raised the groundwater table 3-4 m from the ground level.

The lithology of the landslide site is generally underlain by granitic rock, phyllite and schist (Fig. 4). Most historical landslides occurred on granitic rock formations. Weathering of granitic rock produced residual soil categories Grade V and VI, with a thickness ranging from 15–30 m [18]. These soil deposits consist of residual soil, exhibiting diverse engineering characteristics depending on the extent of weathering. The hydraulic properties of residual soil may differ by as much as two orders of magnitude and correspond with the soil infiltration rate [19].

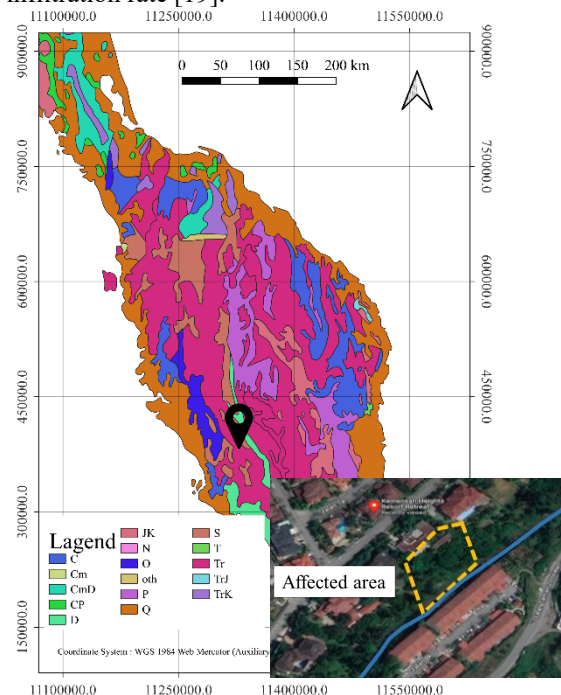


Fig. 1 Location of the landslide



Fig. 2 A photo of the affected area taken two days after the landslide (Source : The Sun)

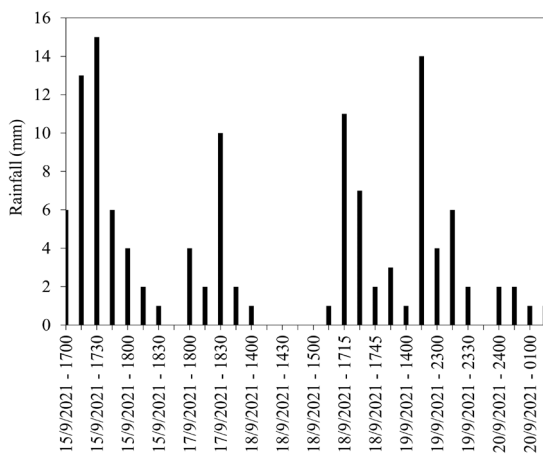


Fig. 3 Rainfall data recorded at the Bukit Antarabangsa station (Source : Department of Irrigation and Drainage Malaysia).

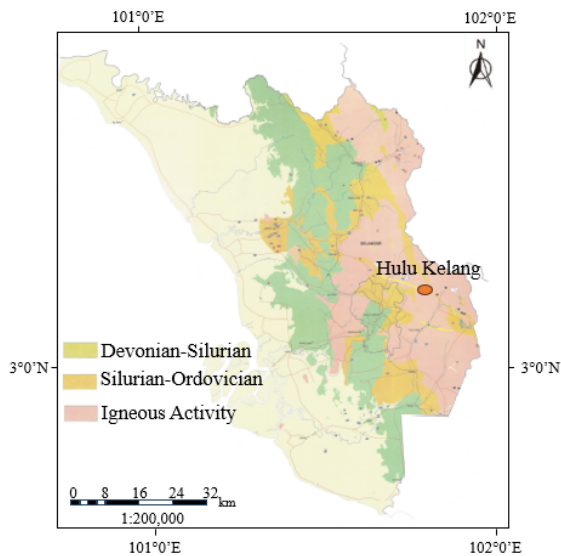


Fig. 4 Lithology of landslide area (Source : Department of Mineral and Geoscience Malaysia)

#### 4. METHODOLOGY

The study method comprised three stages. The first stage comprised a desk study, field observations and investigation, soil sampling and laboratory testing. The second stage was a stability analysis using Plaxis 3D software, and the results were verified with Slope/W software. The final stage determined the factors causing the landslide.

##### 4.1 Desk Study, Field Observation and Investigation, Soil Sampling and Laboratory Tests

The desk study gathered information on the landslide from the open-source data available in the news, the Internet, Google Maps, and other free platforms. The field data collection included TLS surveys, JKR probe testing, and soil sampling. The TLS equipment used in this study was the Leica 360 ScanStation, with an accuracy of  $\pm 0.006$  m at a range of 100 m, to obtain spatial data of the landslide: height, width, and length of the slope. The TLS was placed in front and on the side of the landslide, as shown in Fig. 5. The JKR probe test was conducted at three points: top, middle, and toe of the slope (Fig. 6). The disturbed and undisturbed soil samples were collected using a shovel and split spoon sampler, with a diameter of 50 mm for the triaxial tests and a 110 mm diameter core cutter for the permeability test. All samples were stored in sealed plastic bags to preserve the moisture content. Table 2 lists the types of testing undertaken and the standards used in this study.

Table 2 Field and laboratory testing

Type of testing	Test	Description	Standard / specification
Field	Terrestrial Laser Scanner	Placed at the front and side of landslide	Leica 360, accuracy $\pm 0.006$ m at a range of 100 m
	JKR Probe	Three points (top, middle and bottom)	60-degree cone, 5 kg hammer, 30 cm penetration
Laboratory	CU Triaxial	Undisturbed	BS 1377: 1990, Part 8
	Permeability	Undisturbed	BS 1377: 1990, Part 6
	Sieve Analysis	Disturbed	BS1377:1990, Part 2, Clause 9.5
	Shear box	Undisturbed	BS1377: 1990, Part 2, Clause 8.3
	Soil Density	Disturbed	BS 1377: 1990, Part 4
	Soil compaction Atterberg Limit	Disturbed	BS 1377-4: 1990, Part 4. BS1377: 1990, Part 2, Clause 4

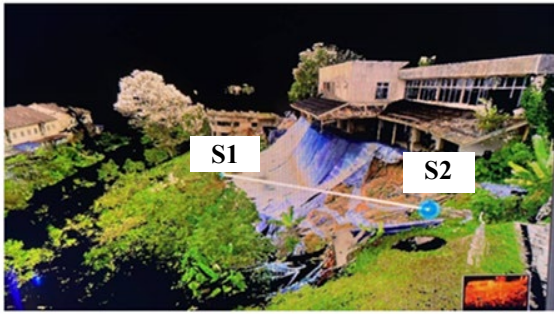


Fig. 5 The positions of the TLS at the site. S1 is at the front and S2 is at the side of the landslide.

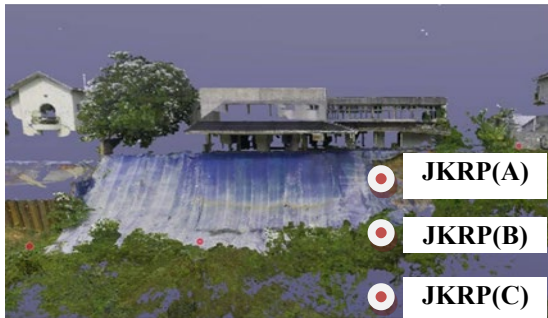
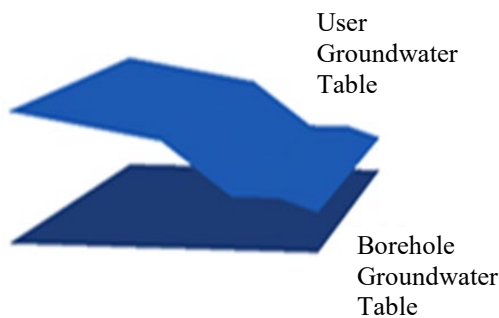


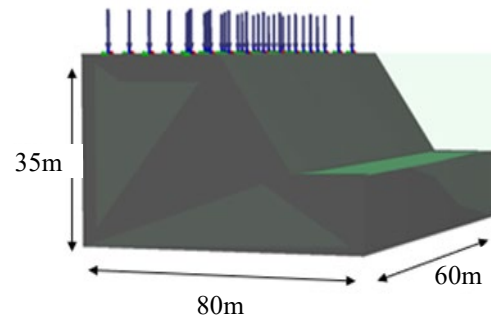
Fig. 6 Locations of the JKR Probe Test conducted on the slope

#### 4.2 Slope Stability Analysis Using Plaxis 3D

Plaxis 3D was used to perform slope stability analysis. The soil was described by a non-linear Hardening Soil Model (HSM). Two levels of groundwater table were used for the flow condition stage: the lower level was a borehole water table located at a depth of 25 m from the ground surface and the upper level was the user-defined water table, located approximately 4 m deep and based on the site investigation conducted by local experts (Fig. 7a). Fig. 7b shows the 3D slope model with a height, length and width of 35, 60, and 80 m, respectively, forming a 35° slope angle. A 50 kPa surcharge load was imposed at the top of the slope to represent the structural load from existing buildings.



(a) Groundwater level input in Plaxis 3D



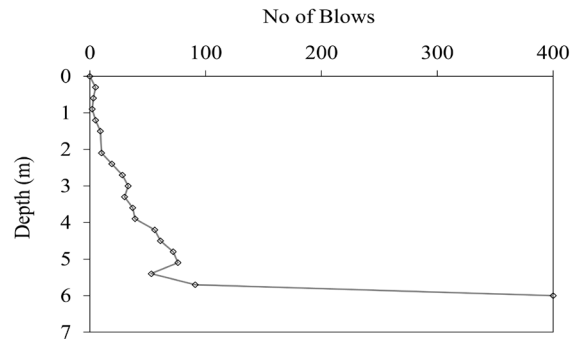
(b) Slope dimension input in Plaxis 3D

Fig. 7 Groundwater table and slope dimension in Plaxis 3D

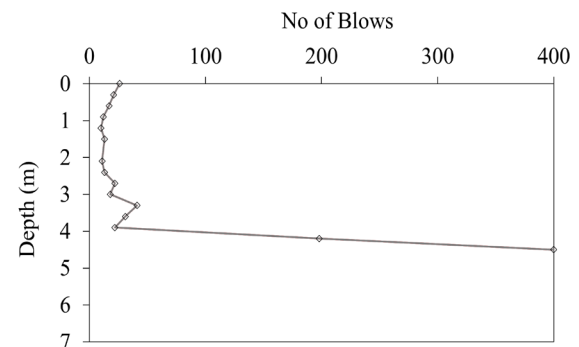
## 5. RESULTS AND DISCUSSION

### 5.1 Field Testing Results

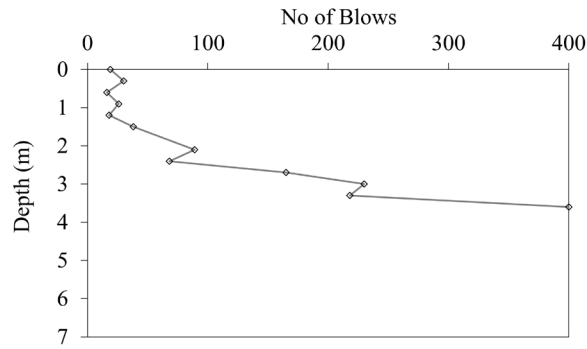
Fig. 8 presents the results of the JKR probe test, at the top, middle and toe of the slope. The schematic cross-section drawing of the slope profile is interpreted using the JKR probe test results shown in Fig. 9. The hard layer measured from the failure plane varies from 3.5-6.0 m. The hard layer could be bedrock or another dense layer. There are distinct soft and hard layers on the slope profile. The depth of the residual soft soil layer is approximately 17-20 m.



(a) Number of blows versus depth for point JKRP(A)



(b) Number of blows versus depth for point JKRP(B)



(c) Number of blows versus depth for point JKRP(C)  
 Fig. 8 The result of the JKR probe test for the top, middle and toe of the slope

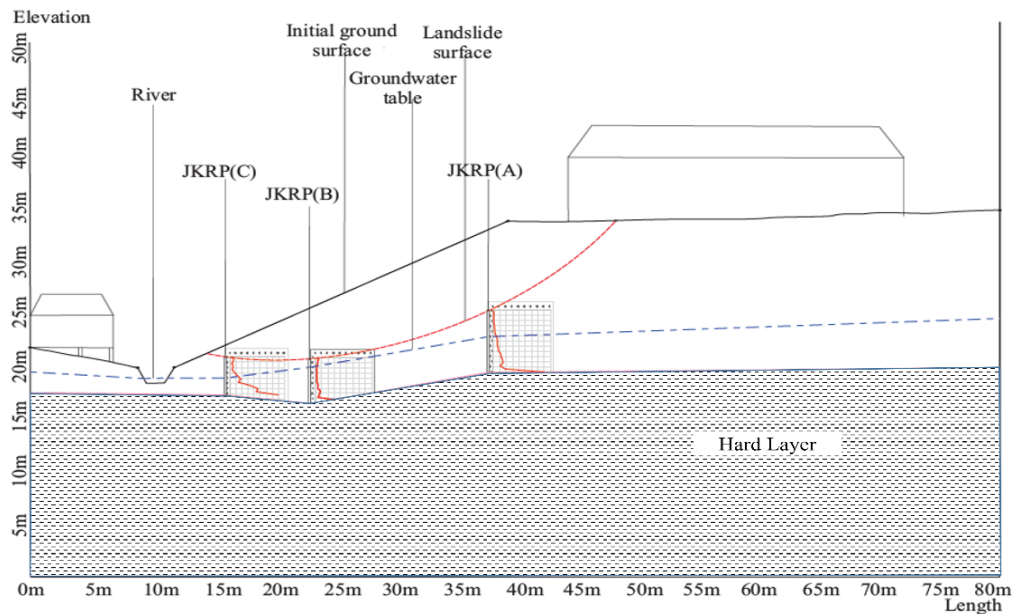


Fig. 9 Schematic drawing of the Kemensah Heights slope.

**5.2 Laboratory Test Results**

**5.2.1 Sieve Analysis and Atterberg Limits**

Fig. 10 shows the results of the sieve analysis. The soil comprises 16% clay, 28% silt, 42% sand and 14% gravel; it is, therefore, classified as silty SAND. The Liquid Limit and Plastic Limit for the soil is 40% and 26%, thus classifying the soil as low plasticity.

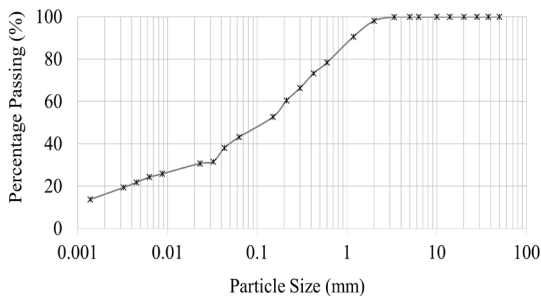


Fig. 10 Particle size distribution

**5.2.2 Permeability and Particle Density**

The average permeability of the soil is  $5.96 \times 10^{-3}$  mm/s, which classifies it as being of medium permeability. The permeability properties play a significant role in rainfall infiltration, potentially increasing the slope's vulnerability to failure. The soil has a particle density of  $2.63 \text{ Mg/m}^3$ .

**5.2.3 Soil Compaction**

Figure 11 shows the result of soil compaction testing, where the maximum dry density of the soil is  $16.51 \text{ kN/m}^3$  at an optimum moisture content of 7.3%.

**5.2.4 Consolidated-Undrained Triaxial Tests (CU)**

The tests were conducted at three confining pressures (50, 100, and 200 kPa) in samples A, B and C (Fig. 12). The cohesion,  $c$ , and angle of internal friction,  $\phi$ , were  $11.3 \text{ kN/m}^2$  and  $29^\circ$ , as determined from the  $t'-s'$  plot shown in Fig. 13.

The soil stiffness parameter,  $E_{50}$ , was

determined from the slope gradient of the stress-strain curve of each sample (see Fig. 14). The average of the slope gradients,  $E_{50}^{ref}$  is 15,835 kPa. The  $E_{ode}^{ref}$  and  $E_{ur}^{ref}$  were calculated using Eq. (1) and Eq. (2). Table 3 summarizes the input strength parameters for the Hardening Soil Model (HSM) obtained from CU triaxial test results.

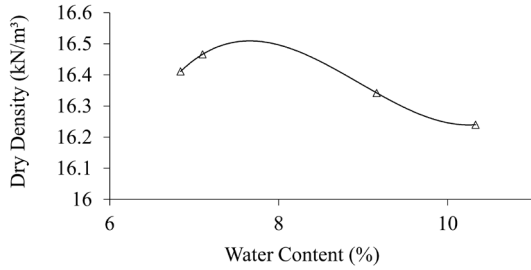


Fig. 11 Soil compaction test results.



Fig.12 Failed samples after CU triaxial testing

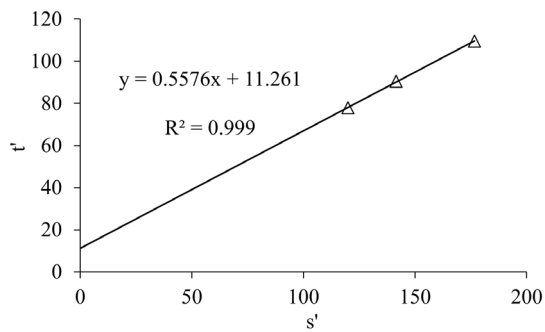
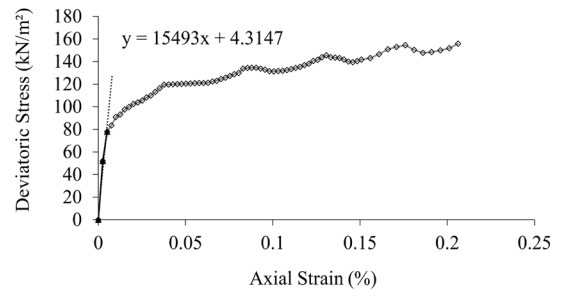
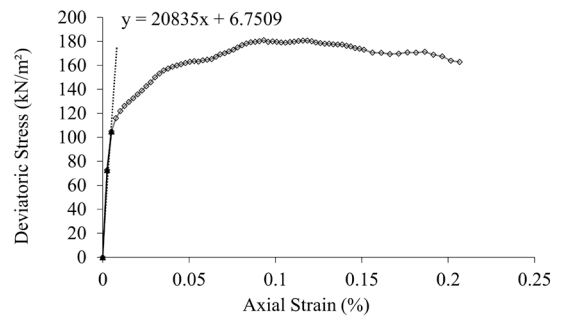


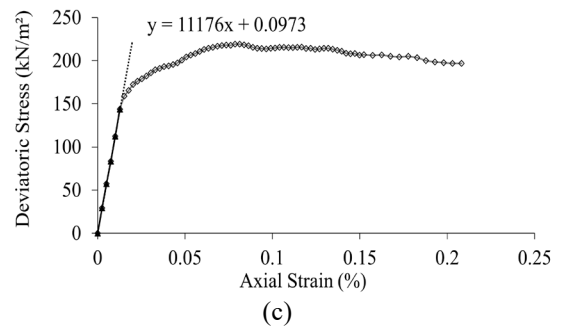
Fig. 13 The shear strength parameters derived from  $t'$ - $s'$  plot



(a)



(b)



(c)

Fig. 14 Determination of the  $E_{50}$  moduli at (a) 50 kPa; (b) 100 kPa; and (c) 200 kPa.

$$E_{ode}^{ref} = \frac{E_{50}^{ref}}{1.25} \tag{1}$$

$$E_{ur}^{ref} = 3 \times E_{50}^{ref} \tag{2}$$

Table 3 The  $E_{50}$ ,  $E_{50}^{ref}$ ,  $E_{ode}^{ref}$ , and  $E_{ur}^{ref}$

Effective major principal stress, $\sigma'_1$ (kPa)	Effective minor principal stress, $\sigma'_3$ (kPa)	$E_{50}$ (kPa)	$E_{50}^{ref}$ (kPa)	$E_{ode}^{ref}$ (kPa)	$E_{ur}^{ref}$ (kPa)
198	42	15493	1583	1268	4750
232	51	20835	5	8	4
286	67	11176			

### 5.3 Plaxis 3D and Slope/W Analysis

Fig. 15 shows the Plaxis 3D results with a factor of safety (FOS) value of 1, indicating that the slope is unstable. The critical slip plane emerged from the crest and intersected the toe of the slope, characterizing the failure line as a toe failure. This result was validated by SLOPE/W and yielded an FOS of 1.095, reaffirming the instability of the slope (see Fig. 16).

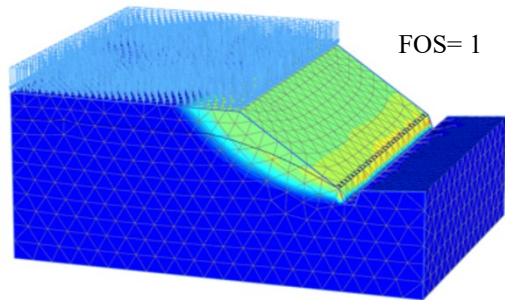


Fig. 15 Result of the Plaxis 3D analysis

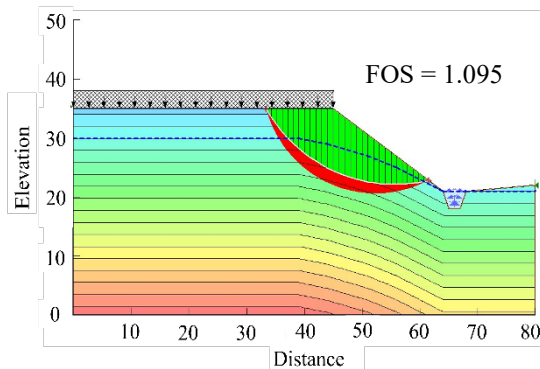


Fig. 16 Result of the Slope/W analysis

### 6. CONCLUSION

There is a variety of factors which trigger landslides. The conclusions drawn from this study are as follows:

Prior to the specific landslide incident being analyzed, heavy rainfall occurred on three consecutive days. Since the permeability of the soil is in the medium range, the antecedent rainfall increased the water infiltration into the soil and, subsequently, increased moisture content, which caused two possible effects: a decrease in the shear strength of the soil and an increase in the overall weight of the soil. The infiltration also caused groundwater level to increase by up to 3-4 m, according to the local experts. The characteristics of the residual soil indicates that it was prone to landslides due to the highly variable engineering

properties, influenced by the degree of weathering.

The laboratory test results showed that the residual soil was categorized as silty sand with low plasticity. It consists primarily of sand (42%), silt (28%), clay (16%) and gravel (14%). The shear strength of the soil is considered low, with a respective cohesion and friction angle of 11.3 kPa and 29°. Meanwhile, the Kemensah Heights have slope angles of approximately 30-35°, higher than the friction angle of the soil. Slope stability is dependent on friction angle and cohesion. In such a situation, with limited shear strength, failure can occur.

Local news reported that there is an excessive imposed load located on the higher ground caused increase shear stress, which can contribute to landslides.

In summary, the key factors triggering the landslide in this case study were the antecedent rainfall, excessive surcharge load (constructed at the edge of the slope) and the characteristics of the residual soil.

### 7. ACKNOWLEDGMENTS

The authors wish to thank the National Defence University of Malaysia for funding and supporting this project under grant, with project code: PS0056UPNM/2022/GPPP/TK/24.

### 8. REFERENCES

- [1] Blasio F.V.D., Introduction to the Physics of Landslides, 1st ed. New York: Springer, 2014.
- [2] Lee M.L., Ng K.Y., Huang Y.F., and Li W.C., Rainfall-Induced Landslides in Hulu Kelang Area, Malaysia. *Nat. Hazards*, Vol. 70, no. 2014, pp.353–375.
- [3] Tran T.V., Pham H.D., Hoang V.H., and Trinh M.T., Assessment of the Influence of the Type of Soil and Rainfall on the Stability of Unsaturated Cut-Slopes—a Case Study. *International Journal of GEOMATE*, Vol. 20, Issue 77, 2021, pp.141–148.
- [4] Arefpanah S. and Sharafi A., Numerical Analysis for Tectonic Activity and Landslide Stability Evaluation in Numerical Analysis for Tectonic Activity and Landslide Stability Evaluation in Baneh, Kurdistan, Iran. *J. Geotech. Geol.*, Vol. 18, no. 1, 2022, pp. 681–686.
- [5] Jelani J., Adnan N.A., Husen H., Mohd D. M.N., and Sojipto S., The Effects of Ground Water Level Fluctuation on Slope Stability by using SlopeW. *Def. Sci. Eng. Technol.*, Vol. 3, no. 1, 2020, pp. 1–7.
- [6] Jelani J., Hah M.S.A., Mohd D.M.N., Ahmad N., Othman M., and Wan M.S.W.M.S., Stability Analysis of a Man-Made Slope: A

- Case Study on the UPNM Campus, Sg Besi, Kuala Lumpur. Sustainable Development of Water and Environment, 2021, pp.39–46.
- [7] Ahmad I.A.S., Jelani J., Wong S.Y., Suif Z., and Ahmad M.A.L., Experimental And Numerical Study On The Behaviour Of Silica Sand Slope Model Subjected To Surcharge Load. *J. Teknol.*, Vol. 86, no. 1, 2024, pp.165-173.
- [8] Emeka A.E., Nnatuanya O.U., Opeyemi A.S., Margaret A.C., and Oduh O.M., Geotechnical and Geological Analysis of Amuzukwu Landslide, *American Journal of Environmental Protection*, Vol. 10, no. 4, 2021, pp.84.
- [9] Popescu M.E., Landslide Causal Factors and Landslide Remedial Options, *The 3rd International Conference on Landslides, Slope Stability and Safety of Infra-Structures*, 2002, pp.61–81.
- [10] Sugawara J., Landslides in Plantation of Tea in Japan, *International Journal of GEOMATE*, Vol. 4, no. 1(SI.7), 2013, pp.495–500.
- [11] Malaysia Among Countries Especially Prone to Landslides, *The Star*, 2018.
- [12] Akter A., Noor M.J.M.M., Goto M., Khanam S., Parvez A., and Rasheduzzaman M., Landslide Disaster in Malaysia: An Overview, *Int. J. Innov. Res. Dev.*, Vol. 8, no. 6, 2019, pp.58-71
- [13] Mukhlisin M., Matlan S.J., Ahlan M.J., and Taha M.R., Analysis of Rainfall Effect to Slope Stability in Ulu Klang, Malaysia, *J. Teknol.*, Vol. 72, no. 3, 2015, pp.15–21.
- [14] Gue S.S. and Liong C.H., Is the Ground in Ulu Klang Unstable? *Jurutera*, 2007, pp. 32–33.
- [15] Samah F.A., Landslides in the Hillside Development in the Hulu Klang, *Post-Graduate Seminar*, 2007, pp. 148–162.
- [16] Mohamad A., Shaharom, S., Mahmud, M., Nik Hassan, N. R., Baba, M. F., Mariappan, S., Huat L.T., Chong S., Madi M.Z., Wan Ishak, W. M. R., Slope Field Mapping and Findings at Ulu Klang Area, Malaysia, *Proceeding of The International Conference on Slopes Malaysia*, 2008, pp. 1–10.
- [17] Huat L.T. and Ibrahim A.S., An Investigation on One of the Rainfall-Induced Landslides in Malaysia, no. December 2008, pp.435–449.
- [18] Faisal A., Unsaturated Tropical Residual Soils and Rainfall Induced Slopes in Malaysia, *Asian Conference on Unsaturated Soils*, 2000, pp.41–52.
- [19] Ng K.Y., Rainfall-Induced Landslides in Hulu Kelang Area, Malaysia, *Universiti Tunku Abdul Rahman*, 2012.

---

Copyright © Int. J. of GEOMATE All rights reserved, including making copies, unless permission is obtained from the copyright proprietors.

---